Computers and Chemical Engineering 95 (2016) 97–107

Contents lists available at ScienceDirect

Computers and Chemical Engineering

journal homepage: www.elsevier.com/locate/compchemeng

Application of a simulated annealing algorithm to design and optimize a pressure-swing distillation process

Yinglong Wang*, Guangle Bu, Yongkun Wang, Tingran Zhao, Zhen Zhang, Zhaoyou Zhu

College of Chemical Engineering, Qingdao University of Science and Technology, Qingdao 266042, China

ARTICLE INFO

Article history:
Received 11 May 2016
Received in revised form 14 July 2016
Accepted 18 September 2016
Available online 20 September 2016

Keywords:
Pressure-swing distillation
Simulated annealing algorithm
Optimization method
Azeotropic mixtures

ABSTRACT

The design and optimization of pressure-swing distillation (PSD) have a critical impact on its economics. An optimization method based on simulated annealing algorithm (SAA) was proposed. The move generator and cooling schedule of the SAA were discussed, and suitable parameter settings were investigated. Two cases of PSD with and without heat integration were optimized by the SAA-based optimization method using procedures of pressure specified and pressure optimized. The results of the process without heat integration were compared with conventional optimization methods. For the acetone-methanol system, the total annual cost (TAC) shows a 5.69% decrease with the pressure specified and a 17.32% decrease with the pressure optimized. For the methanol-chloroform system, the TAC shows a 1.79% decrease with the pressure specified and a 9.04% decrease with the pressure optimized. The SAA-based optimization method has the advantages of a high probability to obtain the global optimum, automatic calculation, and less computing time.

1. Introduction

There are several mixtures that need to be separated in a chemical process industry. Azeotropic mixtures cannot be separated efficiently by conventional distillation (An et al., 2015; Bastos et al., 2015; Mahdi et al., 2014; Skiborowski et al., 2015). To solve this problem, special distillation methods have been proposed, including pressure-swing distillation (PSD) (Lladosa et al., 2011; Luo et al., 2014; Luyben, 2014; Modla et al., 2010; Wang et al., 2015), extractive distillation (Liang et al., 2014; Quijada-Maldonado et al., 2014), and azeotropic distillation (Kunnakorn et al., 2013). PSD is an efficient method to separate pressure-sensitive azeotropic mixtures, whose azeotropic composition clearly changes as the system's pressure changes. PSD has attracted the attention of researchers as it has the advantage of no third component being introduced. Energy consumption and capital investment account for most of the total cost of the PSD process, and the optimization and design of the PSD process have a critical impact on the economics of the entire process (Lladosa et al., 2011).

There are nine design variables to be optimized for a PSD process, including the number of stages (N_{T1}), feed stage location (N_{F1}), recycle stage location (N_{REC}), reflux ratio (RR_1) and pressure (P_1) of column T1; and the number of stages (N_{T2}), feed stage location (N_{F2}), reflux ratio (RR_2), and pressure (P_2) of the column T2. Among them, RR_1, RR_2, P_1 and P_2 are continuous variables, while the others are discrete variables. The optimization of a PSD process is a multiple variable combinatorial optimization problem in which the objective function is the total annual cost (TAC). This type of optimization problem can be formulated as a mixed integer nonlinear programming problem (García-Herreros et al., 2011; Silva and Salcedo, 2011). A sequential iterative method and a heuristic optimization method are commonly used to optimize a PSD in the open literature. For example, Hosgor et al. (2014) optimized a methanol/chloroform system using a sequential iterative method. Luo et al. (2014) optimized an isopropyl alcohol/diisopropyl ether system using a sequential iterative method. Luyben (2008, 2014) optimized a methanol/trimethoxysilane system and an acetone/methanol system using a heuristic optimization method.

Intelligent optimization algorithms, including the simulated annealing algorithm (SAA) (Cheng et al., 2009; Gutiérrez-Antonio et al., 2014; Li et al., 2015; Ochoa-Estopier et al., 2015; Sudibyo et al., 2015; Wang et al., 2012; An and Yuan, 2009), genetic algorithm (Lim et al., 2014; Modla and Lang, 2012), tabu search (Martins and Costa, 2010) and particle swarm optimization (Lahiri, 2014; Liu and Zhao, 2012), have successfully been used in the process design and optimization. SAA is widely used in multi-component distillation sequences (An and Yuan, 2009), heat exchanger net-

* Corresponding author.
E-mail address: yinglongw@126.com (Y. Wang).

http://dx.doi.org/10.1016/j.compchemeng.2016.09.014
0098-1354/

Notation

E	Energy state
$E(X_0)$, $E(X_i)$	Energy state of X_0, X_i
i	Counter variable of movement
i_{min}	Value of the counter i for the minimum TAC state
K	Ratio of the TAC to the energy state function
L	Length of the Markov chain
n	Counter variable of temperature
N_{F1}, N_{F2}	Feed stage location of the column T1, T2
N_{REC}	Recycle stage location of the column T1
N_{T1}, N_{T2}	Total stage of the column T1, T2
P_1, P_2	Pressure of the column T1, T2
PSD	Pressure-swing distillation
RR_1, RR_2	Reflux ratio of the column T1, T2
SA	Simulated annealing
SAA	Simulated annealing algorithm
SAAPSDO	SAA-based pressure-swing distillation optimization
STEP	Maximum step size for each move
T_0	Initial temperature
T_f	Freezing temperature
TAC	Total annual cost [$/y]
VB	Visual basic
X_0	Initial design variables
X_A, X_C, X_M	Purity of acetone, chloroform, and methanol
X_i	Design variables of movement i
α	Temperature decrement factor

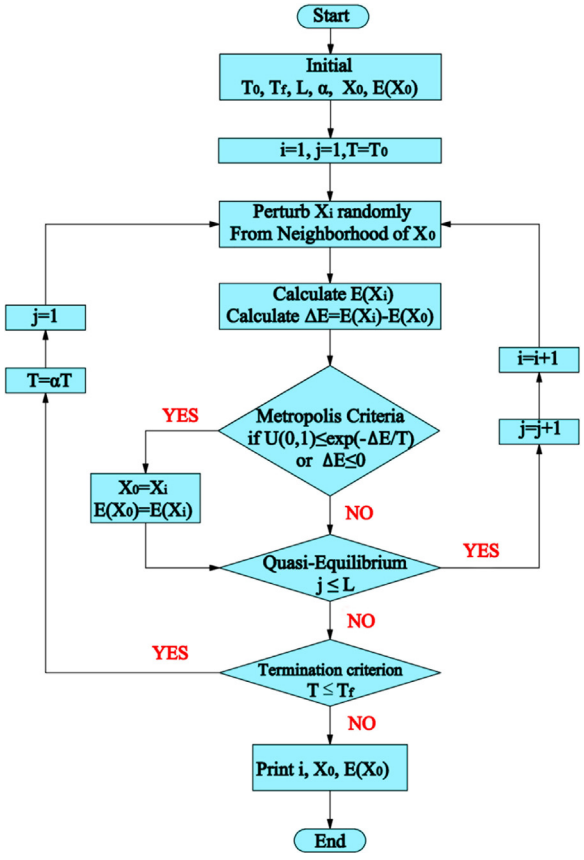

Fig. 1. Flowchart of the simulated annealing algorithm.

work designs (Li et al., 2015; Ochoa-Estopier et al., 2015), phase equilibrium calculations (Zhu et al., 2000), batch distillation process optimizations (Hanke and Li, 2000; Wang et al., 2012), reactive distillation process optimizations (Cardoso et al., 2000; Cheng et al., 2009), azeotropic distillations (Gutiérrez-Antonio et al., 2014), and extractive distillations (García-Herreros et al., 2011). Modla and Lang (2012) optimized a PSD process with a genetic algorithm by minimizing the total annual cost. Simulation-optimization (Chan and Srinivasan, 2016; Silva and Salcedo, 2011) is a special type of optimization technique that makes the use of a simulation to replace deterministic mathematical formulations. The aim of this study is to apply a simulation-optimization technique to the optimization of a PSD by the SAA. The simulation of a PSD process was carried out in Aspen Plus. The simulation-optimization technique was implemented by Visual Basic (VB) interface with Aspen Plus based on the user guide (Aspen Plus User Guide, 2007). To obtain the global optimum of the PSD process, the move generator and the cooling schedule of the SAA will be discussed. Two cases will be studied and different settings for the initial SAA parameters will be attempted until suitable parameters are obtained.

2. Optimal PSD using the SAA

2.1. Simulated annealing

Simulated annealing (SA) (Kirkpatrick et al., 1983) was originally motivated by the process of physical annealing in metal work and successfully used in optimization. SA uses a Metropolis criterion (Metropolis et al., 1953) to have a better chance to obtain the global minimum and escape from being trapped in a local minimum energy state. The flowchart of the simulated annealing algorithm is described in Fig. 1. The energy state (E) is equivalent to the objective function. The parameter settings of the SAA include the initial temperature (T_0), the freezing temperature (T_f), the length of the Markov chain (L), the design variables (X_0), the energy state of X_0 ($E(X_0)$), and the temperature decrement factor (α).

The SA generates a random perturbation that displaces a "particle" (moving the configuration of X_0 to the other configuration, X_i). If the new configuration has a lower energy state, the move is accepted ($X_0 = X_i$, $E(X_i) = E(X_0)$). Otherwise, the move is accepted, with the acceptance probability of the Metropolis criterion shown as Formula (1).

$$P = exp\left(-\frac{E(X_i) - E(X_0)}{K_b T}\right) = exp\left(-\frac{\Delta E}{T}\right) \quad (1)$$

The counter (i) adds one when the inner loop is executed. The outer loop is executed when the counter (i) is larger than the length of the Markov chain (L). If the temperature (T) reaches the freezing temperature (T_f), then the optimal design (X_0) and the energy state ($E(X_0)$) are obtained.

2.2. Parameters of the SAA

To obtain the global optimum of the PSD process, the move generator and cooling schedule should be determined. Hanke and Li (2000), Zhu et al. (2000), and Cheng et al. (2009) discussed the cooling schedule of the SAA, which includes the initial temperature (T_0), temperature decrement, length of the Markov chain (L) and termination criterion.

2.2.1. Move generator

(a) Discrete variables: $X_i = X_0 + Int\{[2U(0,1) - 1] \times STEP\}$, where $MinVal \le X_i \le MaxVal$

(b) Continuous variables: $X_i = X_0 + \text{Round}\{[2U(0,1) - 1] \times \text{STEP}, 2\}$, where $\text{MinVal} \le X_i \le \text{MaxVal}$

STEP means the maximum step sizes for each move, Int indicates that the number is rounded off, Round (x, 2) means rounded x to two decimal places, U(0,1) indicates a uniform distribution for the interval (0, 1), MaxVal denotes the maximum value of X_i, and MinVal means the minimum value of X_i.

The number of stage and feed stage locations of the distillation column are discrete variables that use move generator (a). The design variables for pressure and reflux ratio are continuous variables that use move generator (b).

2.2.2. Initial temperature (T_0)

The initial temperature should be large enough to find the global optimum. However, a higher initial temperature results in a larger computing time. The choice of the initial temperature value should essentially be that all new configurations are accepted virtually according to the Metropolis criterion for the initial temperature, and the acceptance ratio (the ratio of the number of accepted configurations to the total number of new configuration) decreases as the temperature decreases. Before selecting the initial temperature, a suitable value of K (the ratio of the TAC to the energy state function) must be specified first. The aim of setting the factor K is to find other cooling schedule parameters easily, and it is not affected by the system of the PSD. The criterion for the determination of the initial temperature is as following.

The temperature is set as $50 \le T_0 \le 500$, and the acceptance ratio is approximately 100% at a temperature of T_0. Three hundred moves are attempted, and the number of accepted configurations and acceptance ratio are calculated by the SAAPSDO software. If the acceptance ratio is between 90% and 95%, T_0 is suitable for the system of the PSD. If not, the value of T_0 is adjusted until the acceptance ratio achieves the requirement.

2.2.3. Temperature decrement

The temperature decrement is crucial for the convergence and performance of the SA method. If the cooling rate is too slow, the computing time will become very large. If the cooling rate is too fast, the SAA may escape from the global optimum, which results in being trapped in a local optimum. The criterion of the geometry temperature decrement (Kirkpatrick et al., 1983) is used to control the speed of the temperature decrement.

$$T_{n+1} = \alpha T_n,$$

where $0.80 \le \alpha \le 0.99$ (α is temperature decrement factor and n is the counter of the temperature).

2.2.4. Length of the Markov chain (L)

The number of new configurations (X_i) attempted at any specific temperature (T_n) is the length of the Markov chain (L_n). The temperature, T_n, decreased after the L_n step length adjustments, completing a "Markov chain" in the outer loop. The length of the Markov chain must be long enough for the system to reach a steady quasi-equilibrium state at each temperature, which can be determined by the neighborhood configurations obtained in only one movement starting from stage i in all directions (Zhu et al., 2000). A movement of discrete variables results in TAC changes that are significantly larger than the continuous variables, and the effect of variable changes in a different system are different. For the optimization of the PSD, there are nine design variables to be optimized, and each variable has two directions (i.e., increase and decrease) at each temperature. Therefore, the length of the Markov chain of each temperature can be defined as a value of L, which can be assumed to be a value of approximately eighteen based on instinct.

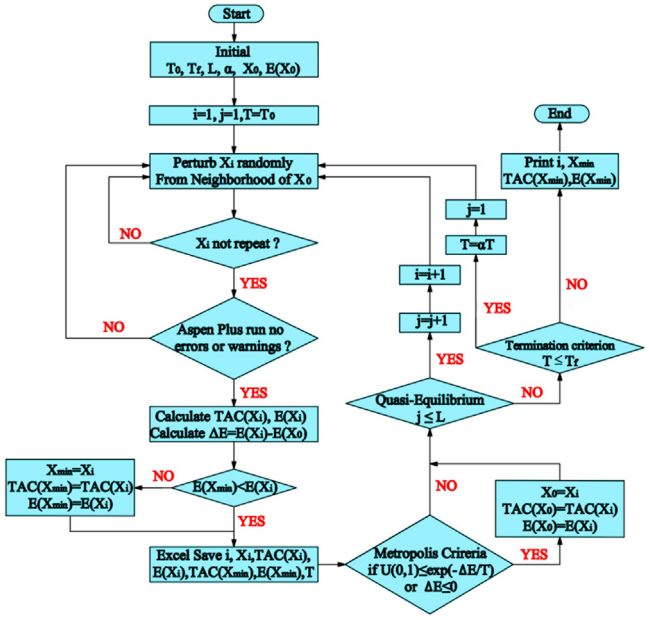

Fig. 2. Flowchart of the SAA implementation for the optimization of the PSD process.

2.2.5. Termination criterion

The SAA termination criterion frequently uses the freezing temperature (T_f), namely, the annealing process terminates when the temperature comes to the freezing temperature. The temperature of the SAA must approach a value of zero as the algorithm progresses. In practice, the temperature value is reduced to sufficiently small values such that virtually no worse configurations are accepted according to the Metropolis criterion and no further significant improvement of the objective function is expected. The temperature changed 138 times from 200 down to 0.0001, with an α of 0.9, which is sufficient to obtain the optimal solution. Therefore, the freezing temperature is set as a value of 0.0001.

2.3. Optimizing the PSD using the SAA

Three judgment modules and a data memory module are added when implementing the SAA to optimize the PSD process. The algorithm flowchart of the SAAPSDO software is shown in Fig. 2. A repeated judgment module is added to avoid the same variable (X_i) calculations in the run of the SAAPSDO software. An Aspen Plus run errors judgment module is added to warn of running errors or warn of design variables that are generated randomly in a certain range. The minimum judgment module is added such that the change in the minimum TAC and the values of the design variables can be easily found. The rules for changing the minimum configuration as the temperature decreases can be investigated. A data memory module is added by interfacing with Microsoft Office Excel to save the data for the design variables, TAC values of the PSD, annealing temperatures, and so on.

The present SAA-based optimization method was carried out by the SAA-based Pressure-Swing Distillation Optimization (SAAPSDO) software. The software is implemented by software integration of VB interfaces with Aspen Plus and Microsoft Office Excel. The main interface and the "Total Annual Cost Model" interface were designed in a manner such that all necessary parameters of the SAA, PSD, and TAC formulae can be specified, which are shown in Figs. 3 and 4. Clicking the menu "TACModel" will go to the "Total Annual Cost Model" interface, and the TAC model can be specified in the "Total Annual Cost Model" interface. In this study, the TAC model follows the basic economic model of Luyben (2013).

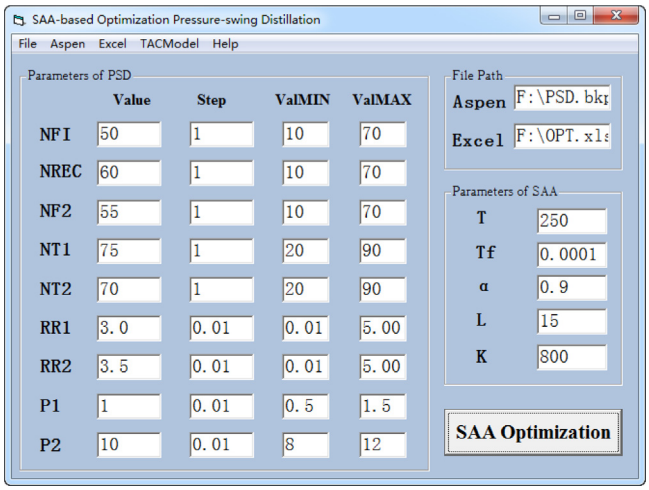

Fig. 3. Main interface of the SAA-based pressure-swing distillation optimization software.

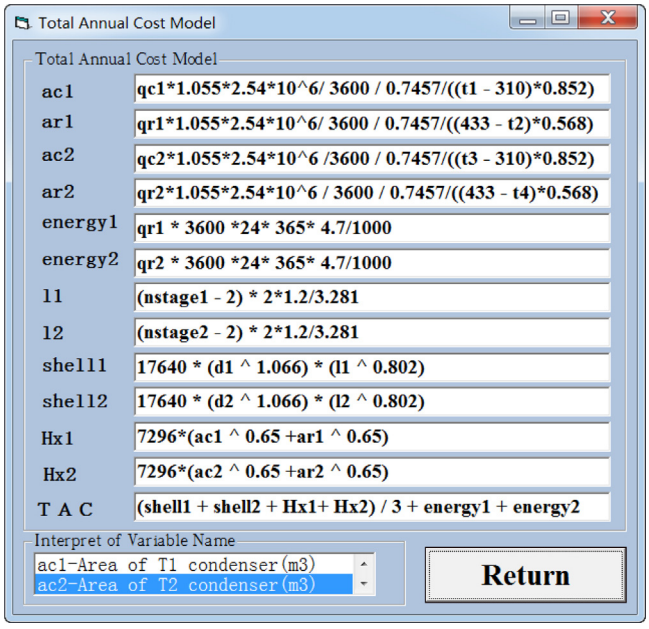

Fig. 4. Interface of the "Total Annual Cost Model" of the SAAPSDO software.

The optimization procedure of the SAA consists of the following steps, as shown in Fig. 2. The initial values and constraints of the nine PSD design variables, parameters of the SAA, path of Excel, path of Aspen Plus and the TAC model were specified first. Then, the values of the nine design variables were generated. The values of N_{T1}, N_{T2}, N_{F1}, N_{REC}, and N_{F2} were randomly generated according to the discrete variables move generator. The values of design variables RR_1, RR_2, P_1, and P_2 were randomly generated according to the continuous variables move generator. The values of the design variables were searched to avoid repetition and then transferred to Aspen Plus for the process simulation. The process simulation running errors were judged by interfacing with the Aspen Plus running history file. The results without errors or warnings were transferred back to the SAAPSDO software to calculate the TAC and the energy state (1/K times of the TAC). Microsoft Office Excel was interfaced with to save the calculated results, including the optimized results. The steps above were repeated until the SAA met the termination criterion. The optimum design and minimum TAC were

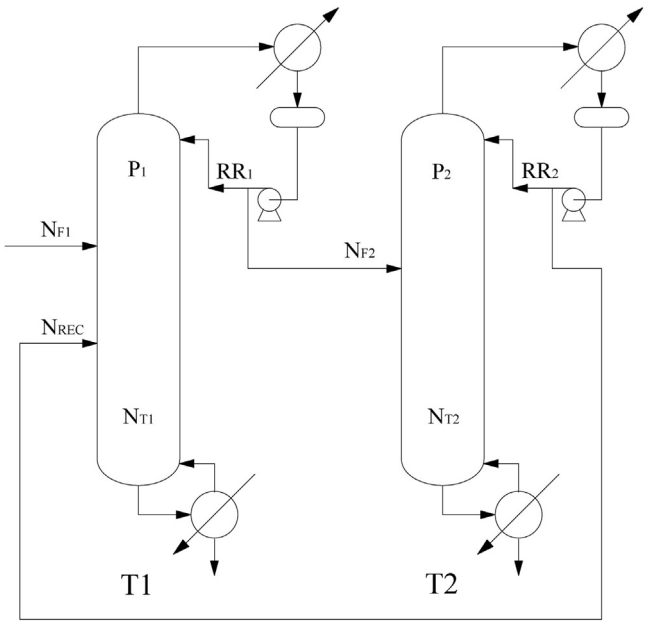

Fig. 5. Scheme of the pressure-swing distillation process with the design variables optimized.

obtained after the procedure of optimization finished. A portion of the SAAPSDO software code is listed in the Appendix A.

3. Case studies

Heuristic optimization and the sequential iterative optimization method are widely used in the optimization of a PSD. Luyben (2008) used a heuristic optimization method to design a PSD process for separating acetone-methanol, and the minimal TAC of the optimized system was calculated. Hosgor et al. (2014) used a sequential iterative optimization method to find the optimal design of a PSD for separating a methanol-chloroform azeotrope by minimizing the TAC. In this paper, the above mentioned two PSD processes for acetone-methanol and methanol-chloroform separation are re-optimized with the SAA optimization method to make a comparison with the conventional optimization methods.

The design variables of the PSD process to be optimized are shown in Fig. 5. These design variables are optimized by generating a random perturbation in their constraints based on the SAA optimization method. The pressures in the two columns of the PSD can obtain more precise optimum values using the SAA-based optimization method compared with the conventional optimization methods that are based on the T-xy curves of azeotropic mixtures at different pressures. In studies of Luyben (2008) and Hosgor et al. (2014), the distillate composition specification of columns generally set a fixed value that was lower or higher than the azeotropic composition. The fixed value was specified in their studies but was optimized in our studies, so the TAC calculated by the conventional optimization methods in our studies is lower than the paper's TAC. For example, the TAC for separating acetone-methanol (Luyben, 2008) based on the conventional optimization methods is 4,187,195 $/yr rather than 4,520,000 $/yr which was reported in the cited paper.

3.1. Acetone-methanol system

3.1.1. No heat integration

The steady-state flowsheet of the PSD for separating the acetone-methanol mixture can be found in the study of Luyben (2008). The bottom purities (X_M = 99.5 mol% and X_A = 99.4 mol%)

Table 1
Test results using different initial temperatures for the acetone-methanol system.

T_0	Acceptance ratio
100	83.8%
150	86.9%
200	89.4%
250	91.3%

Table 2
Initial values of the PSD design variables for the acetone-methanol system.

Run	N_{T1}	N_{F1}	N_{REC}	RR_1	P_1	N_{T2}	N_{F2}	RR_2	P_2	TAC
A	70	55	55	3.0	1	70	55	3.0	10	4,450,759
B	75	50	60	3.0	1	70	55	3.5	10	4,398,284
C	75	60	55	3.0	1	80	50	3.0	10	4,433,552

are achieved by adjusting the bottom rate using the "Design Spec/Vary" feature of Aspen Plus. The constraints on the design variables were specified as $20 \le N_{T1} \le 90$, $10 \le N_{F1} \le 70$, $10 \le N_{REC} \le 70$, $0.01 \le RR_1 \le 5.00$, $20 \le N_{T2} \le 90$, $10 \le N_{F2} \le 70$, $0.01 \le RR_2 \le 5.00$, $0.5 \le P_1 \le 1.5$, and $8 \le P_2 \le 12$.

The published paper (Luyben, 2008) determined the pressures in the two columns based on the T-xy curves of the azeotropic mixtures at different pressures, which were not optimized. The optimization of the PSD process by the conventional method usually contains seven design variables, except pressure. To compare the SAA-based optimization method with the conventional method and find the effect of pressure on the TAC of the PSD processes, two procedures were executed for the optimization of the PSD processes. One of them is pressure specified and the other is pressure optimized; the procedure with the pressure specified was executed first.

The acceptance ratios for different initial temperatures are shown in Table 1. The acceptance ratio reaches 83.8% at $T_0 = 100$. Setting a higher initial temperature (T_0) is helpful for the optimization of the SAA to obtain the global optimal design. The initial temperature (T_0) was determined to be 250 with an acceptance ratio of 90% to 95%.

To obtain more general parameter settings for the SAA, three different runs (Run A–C) with different initial values of the design variables (X_i) were tested (Table 2). The initial values of the design variables (X_i) were chosen randomly as long as the TAC of the initial design was large enough. Four different subcases (subcases 1–4) were used to illustrate the choice of the SAA parameter settings, such as α, L, and STEP. The optimization results with different parameter settings for the SAA are shown in Table 3. The results show that only by using the parameter settings of the SAA in subcase 4 Run A–C was able to obtain the global optimum TAC. The

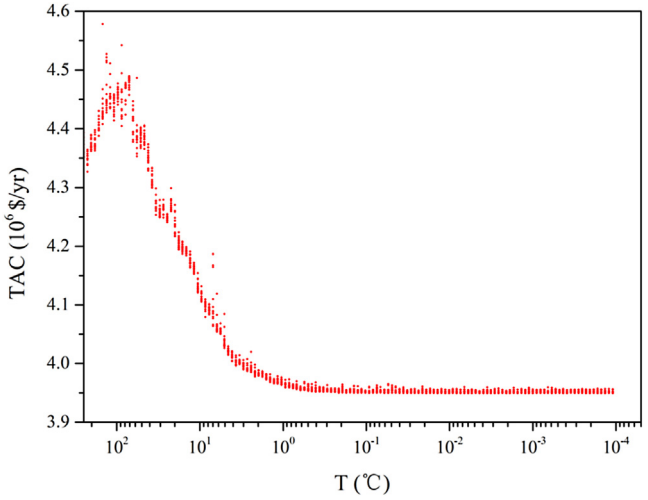

Fig. 6. The result of the annealing process for the acetone-methanol system with the initial settings of run B in subcase 4.

annealing process with different initial values of the PSD design variables results in the same optimum design, which demonstrated that the result is reliable. The STEP of 1 has a good performance compared with the STEP of 2. The STEP of 1 generates a smaller scale random perturbation and can generate a lower TAC when the temperature is low. An α of 0.9 has a better performance compared with an α of 0.8. Markov chain length of 15 is sufficient for the cooling process to reach quasi-equilibrium at each temperature. Therefore, the parameters of the SAA are determined as STEP = 1, $T_0 = 250$, α = 0.9, L = 15, $T_f = 0.0001$, and K = 800.

The results of the annealing process with the initial settings of run B in subcase 4 are shown in Fig. 6. To compare runs of different initial design variables with each other, the TAC of each temperature is contrasted with the average TAC value of that temperature. The results for subcase 4 with three different runs are shown in Fig. 7(a). The results reveal that the TAC decreases and the global optimum TAC is obtained as the temperature decreases. The design variable parameters and economics of the optimum results based on the conventional method and the SAA method are shown in Table 4. The minimum TAC obtained by the SAA-based optimization method with the pressure specified is 3,949,133 $/yr, which is a decrease of 5.69% compared with the heuristic optimization method (4,187,195 $/yr).

A similar procedure with nine design variables (including pressure) of the PSD process is optimized after the optimum design with the pressure specified was obtained. The initial design variable (X_i)

Table 3
The optimization results of the acetone-methanol system using different parameter settings for the SAA.

Subcase	T_0	T_f	α	L	STEP	Run	TAC ($/y)	Dev.[a]	Computing time (h)[b]
1	250	0.0001	0.8	10	2	A	3,987,694	9.76‰	0.3
						B	3,982,097	8.35‰	0.3
						C	3,978,770	7.51‰	0.3
2	250	0.0001	0.8	10	1	A	3,956,189	1.79‰	0.3
						B	3,960,948	2.99‰	0.3
						C	3,965,264	4.09‰	0.3
3	250	0.0001	0.9	10	1	A	3,949,133	0‰	0.7
						B	3,949,133	0‰	0.7
						C	3,949,295	0.04‰	0.7
4	250	0.0001	0.9	15	1	A	3,949,133	0‰	1.0
						B	3,949,133	0‰	1.0
						C	3,949,133	0‰	1.0

[a] Deviation from the optimum TAC obtained (TAC = 3,949,133 $/y).
[b] Microprocessor: Intel Core i7-3770 CPU @ 3.40 GHz.

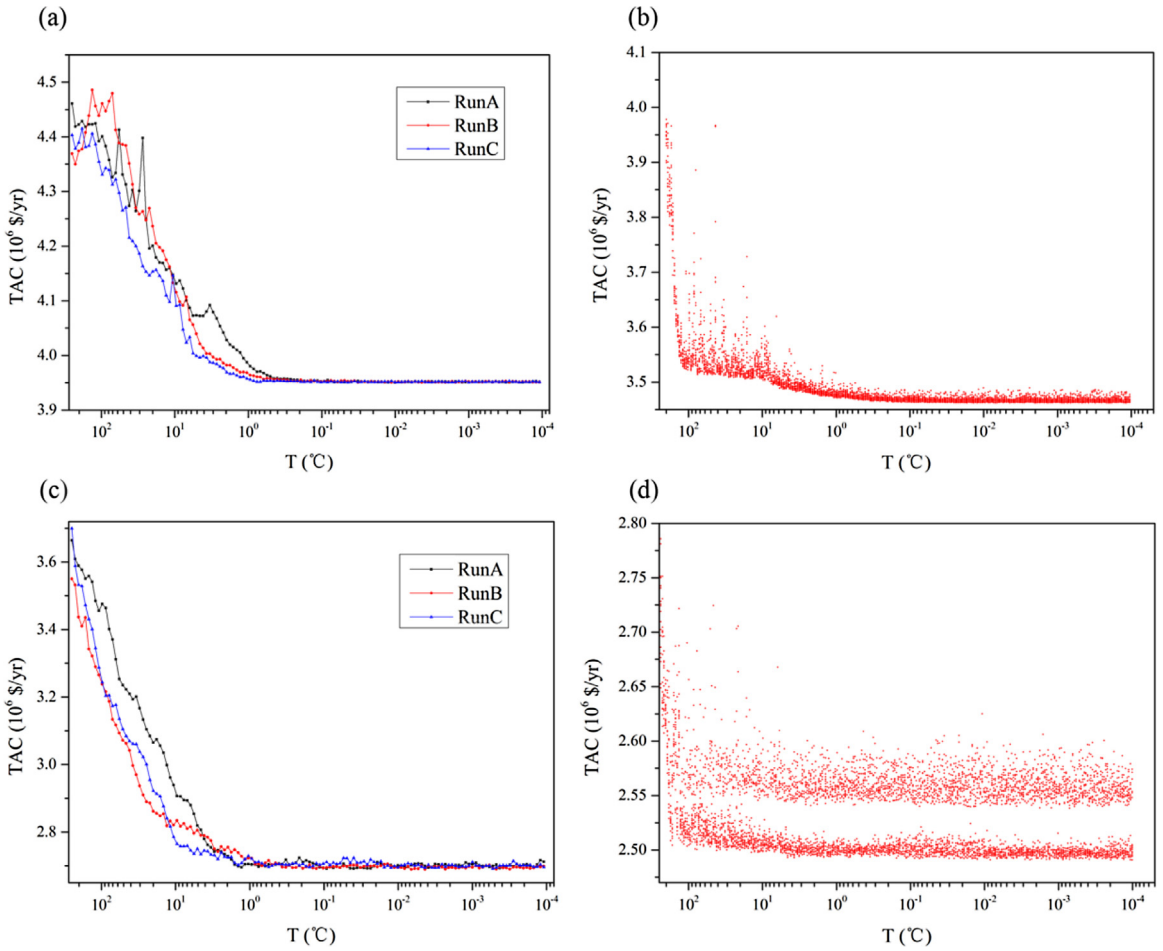

Fig. 7. The annealing processes for the acetone-methanol system: (a) No heat integration with the pressure specified. (b) No heat integration with the pressure optimized. (c) Partial heat integration with the pressure specified. (d) Partial heat integration with the pressure optimized.

settings of the PSD process adopt the optimum design of the SAA-based optimization method with the specified pressure. There are nine design variables for the optimization procedure with the optimized pressure, and the length of the Markov chain (L) and the temperature decrement factor (α) of the SAA should be increased. The parameters of L and α for the pressure optimized procedure are altered to 20 and 0.95. The annealing process with the pressure optimized is presented in Fig. 7(b) and shows that the TAC decreases as the temperature decreases. The optimum design and economics presented in Table 4 show that the TAC decreases to 3,461,941 $/yr, which is a decrease of 17.32% compared with the heuristic optimization method (4,214,998 $/yr). The composition profiles of the two distillation columns are shown in Fig. 8(a) and (b).

Table 4
The optimum design and TAC of the PSD with no heat integration to separate acetone-methanol.

	Conventional	SAA (pressure specified)	SAA (pressure optimized)
N_{T1}	52	45	38
N_{F1}	37	29	25
N_{REC}	42	37	31
RR_1	2.84	1.9	1.72
P_1 (atm)	1	1	0.62
N_{T2}	62	55	51
N_{F2}	41	37	33
RR_2	3.11	2.98	3.14
P_2 (atm)	10	10	11.11
TAC ($/y)	4,187,195	3,949,133	3,461,941
Decrease	–	5.69%	17.32%
Computing time (h)	–	1.0	2.75

3.1.2. *Partial heat integration*

The calculation of the TAC for the partial heat integration process is determined for the condenser heat duty of the high-pressure column and the reboiler heat duty of the low-pressure column. If the former is higher than the latter, an auxiliary condenser will be added. If the opposite, then an auxiliary reboiler will be added. Therefore, a TAC calculation for these two different situations is set and a judgment module is added.

Two procedures were executed for the optimization of the partial heat integration process, where one of them is pressure specified and the other is pressure optimized. The parameters of the SAA with the pressure specified are set as: STEP = 1, T_0 = 250, α = 0.9, L = 20, T_f = 0.0001, and K = 800. A solution without further optimization was used as a comparison, which was the design of the optimum value of the pressure specified process without heat integration optimized by the SAA-based optimization method. The optimum design and economics for the partial heat integration process are given in Table 5. The composition profiles of the two distillation columns of the optimized solution with the pressure optimized are shown in Fig. 8(c) and (d). The annealing processes of these procedures are shown in Fig. 7(c) and (d). The results reveal that the minimum TAC is obtained as the temperature decreases. There are two trends for the optimization of the partial heat integration process, as presented in Fig. 7(b): one decreases

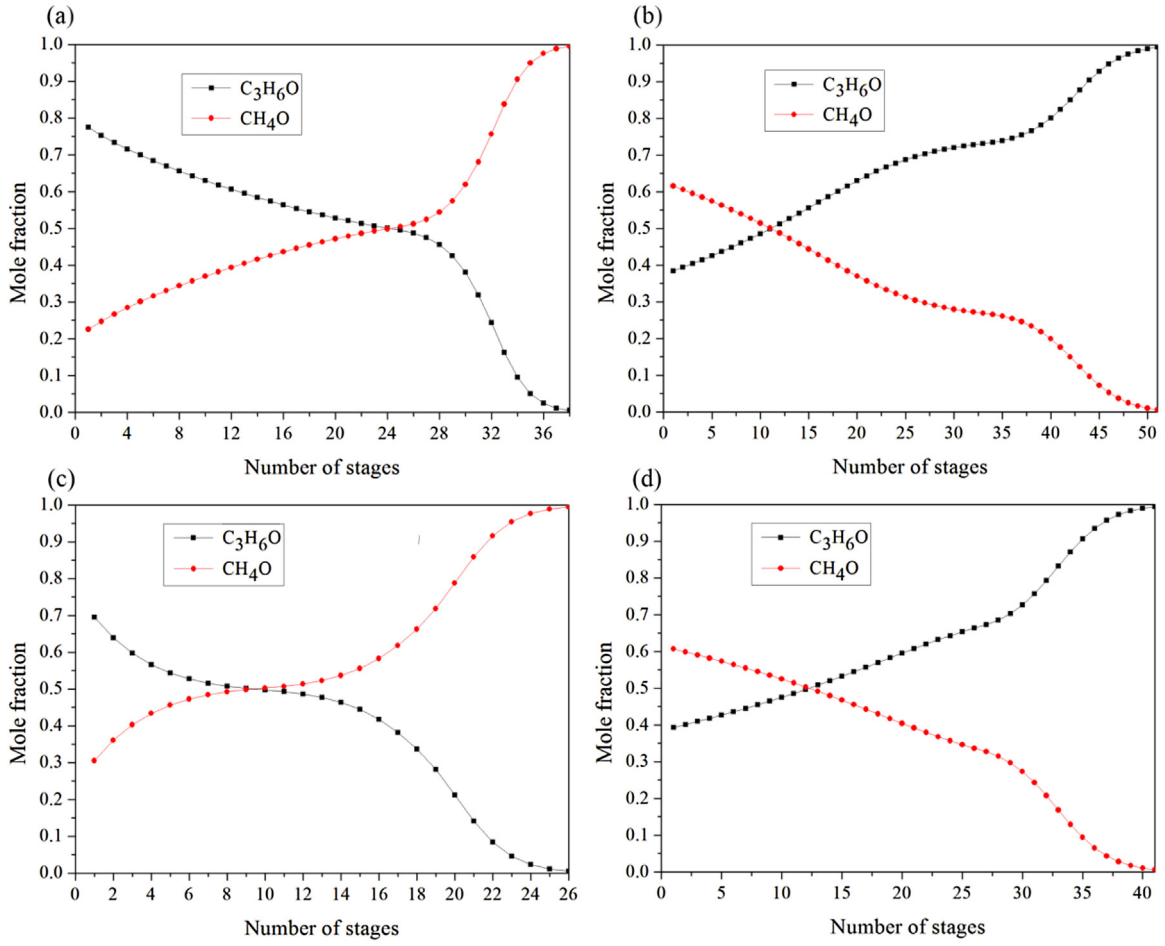

Fig. 8. Composition profiles for the acetone-methanol system: (a) Column T1 with no heat integration. (b) Column T2 with no heat integration. (c) Column T2 with partial integration. (d) Column T2 with partial heat integration.

Table 5
The optimum design and TAC of the PSD with partial heat integration to separate acetone-methanol.

	Conventional	SAA (pressure specified)	SAA (pressure optimized)
N_{T1}	45	30	26
N_{F1}	29	12	10
N_{REC}	37	22	19
RR_1	1.9	1.13	0.94
P_1 (atm)	1	1	0.66
N_{T2}	55	46	41
N_{F2}	37	32	27
RR_2	2.98	3.3	3.12
P_2 (atm)	10	10	10.32
TAC ($/y)	2,948,466	2,683,013	2,490,877
Decrease	–	9.00%	15.52%
Computing time (h)	–	1.3	2.8

Table 6
Initial values of the PSD design variables for the methanol-chloroform system.

Run	N_{TI}	N_{F1}	N_{REC}	RR_1	P_1	N_{T2}	N_{F2}	RR_2	P_2	TAC
A	34	22	22	1.2	1	33	25	1.4	10	890,273
B	36	30	30	1	1	36	30	1	10	967,082
C	28	20	17	0.6	1	31	26	1	10	853,094

to approximately 2,550,000 $/yr and the other one decreases to approximately 2,500,000 $/yr. We assumed that this is caused by the calculation of the TAC for the two different situations of the partial heat integration process. This assumption was demonstrated to be true by checking the original data in Fig. 7(d).

3.2. Methanol-chloroform system

3.2.1. No heat integration

The steady-state flowsheet of the PSD to separate the methanol-chloroform mixture can be found in the study of Hosgor et al. (2014). The bottom purities (X_M = 99.5 mol% and X_C = 99.5 mol%) are achieved by adjusting the bottom rate. The constraints on the design variables are specified as $1 \le N_{T1} \le 50$, $1 \le N_{F1} \le 40$, $1 \le N_{REC} \le 40$, $0.01 \le RR_1 \le 2.00$, $1 \le N_{T2} \le 50$, $1 \le N_{F2} \le 40$, and $0.01 \le RR_2 \le 2.00$, $0.5 \le P_1 \le 1.5$, $8 \le P_2 \le 12$.

A procedure with the pressure specified is executed, and different initial values for the design variables (X_i) for the PSD process are tested (Table 6). As with the previous example, different parameter settings of the SAA were tested. The initial temperature (T_0) is determined to be 200, with an acceptance ratio between 90% and 95%. The other settings for the SAA are: STEP = 1, α = 0.9, L = 18, T_f = 0.0001, and K = 500. The pressures in the two columns are optimized based on the above optimum design. The annealing processes of these procedures are shown in Fig. 9(a) and (b). The optimum design and economics of these procedures are shown in Table 7. The composition profiles for the two distillation columns are shown in Fig. 10(a) and (b).

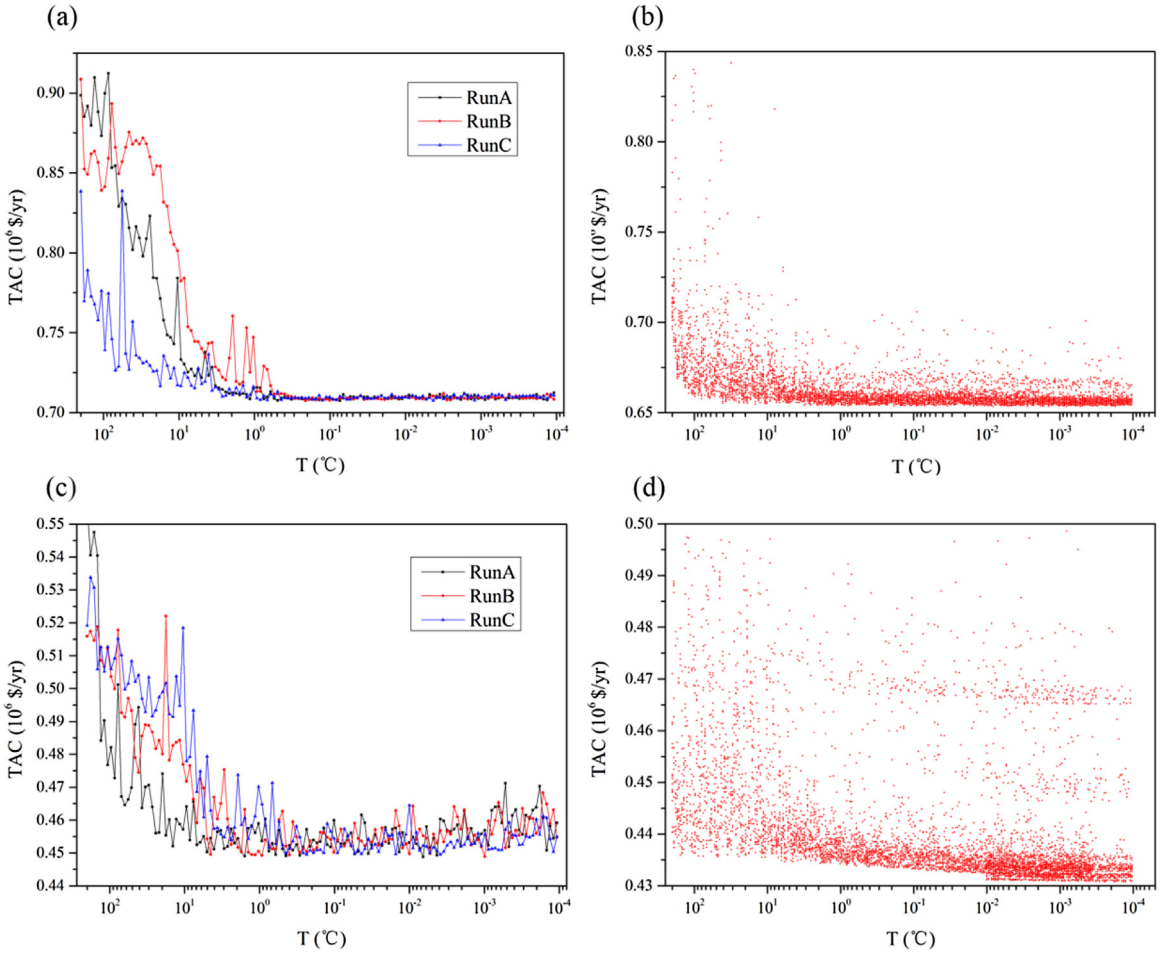

Fig. 9. The annealing processes for the methanol-chloroform system: (a) No heat integration with the pressure specified. (b) No heat integration with the pressure optimized. (c) Full heat integration with the pressure specified. (d) Full heat integration with the pressure optimized.

3.2.2. *Full heat integration*

The steady-state flowsheet of the PSD with full heat integration to separate a methanol-chloroform mixture can be found in the study of Hosgor et al. (2014). A similar optimization procedure was executed. The parameters of the SAA are set as: STEP = 1, T_0 = 200, α = 0.9, L = 20, T_f = 0.0001, and K = 500. The temperature decrement factor (α) was set as 0.95 for the optimization procedure with the pressure optimized. The annealing process and results are shown in Fig. 9(c) and (d), and Table 8. The composition profiles for the two distillation columns of the optimized solution with the pressure optimized are shown in Fig. 10(c) and (d). The optimum values of the design variables for the methanol-chloroform system are substantially smaller than those of the acetone-methanol system. For the methanol-chloroform system, a larger TAC can be generated with a small random perturbation of the optimum design. Therefore, several larger TAC designs can be generated, and the data are dispersed around the freezing temperature in Fig. 9(c) and (d).

Table 7
The optimum design and TAC of PSD with no heat integration to separate methanol-chloroform.

	Conventional	SAA (pressure specified)	SAA (pressure optimized)
N_{T1}	24	20	19
N_{F1}	9	7	7
N_{REC}	18	12	12
RR_1	0.55	0.46	0.43
P_1 (atm)	1	1	0.71
N_{T2}	25	19	17
N_{F2}	20	14	12
RR_2	0.95	0.73	0.72
P_2 (atm)	10	10	10.88
TAC ($/y)	718,449	705,574	653,479
Decrease	–	1.79%	9.04%
Computing time (h)	–	1.2	2.7

Table 8
The optimum design and TAC of PSD with full heat integration to separate methanol-chloroform.

	Conventional	SAA (pressure specified)	SAA (pressure optimized)
N_{T1}	20	18	16
N_{F1}	7	9	8
N_{REC}	12	11	11
RR_1	0.46	0.81	0.74
P_1 (atm)	1	1	0.79
N_{T2}	19	17	17
N_{F2}	14	13	12
RR_2	0.73	–	–
P_2 (atm)	10	10	10.89
TAC ($/y)	448,954	447,161	430,779
Decrease	–	0.40%	4.05%
Computing time (h)	–	1.3	3.2

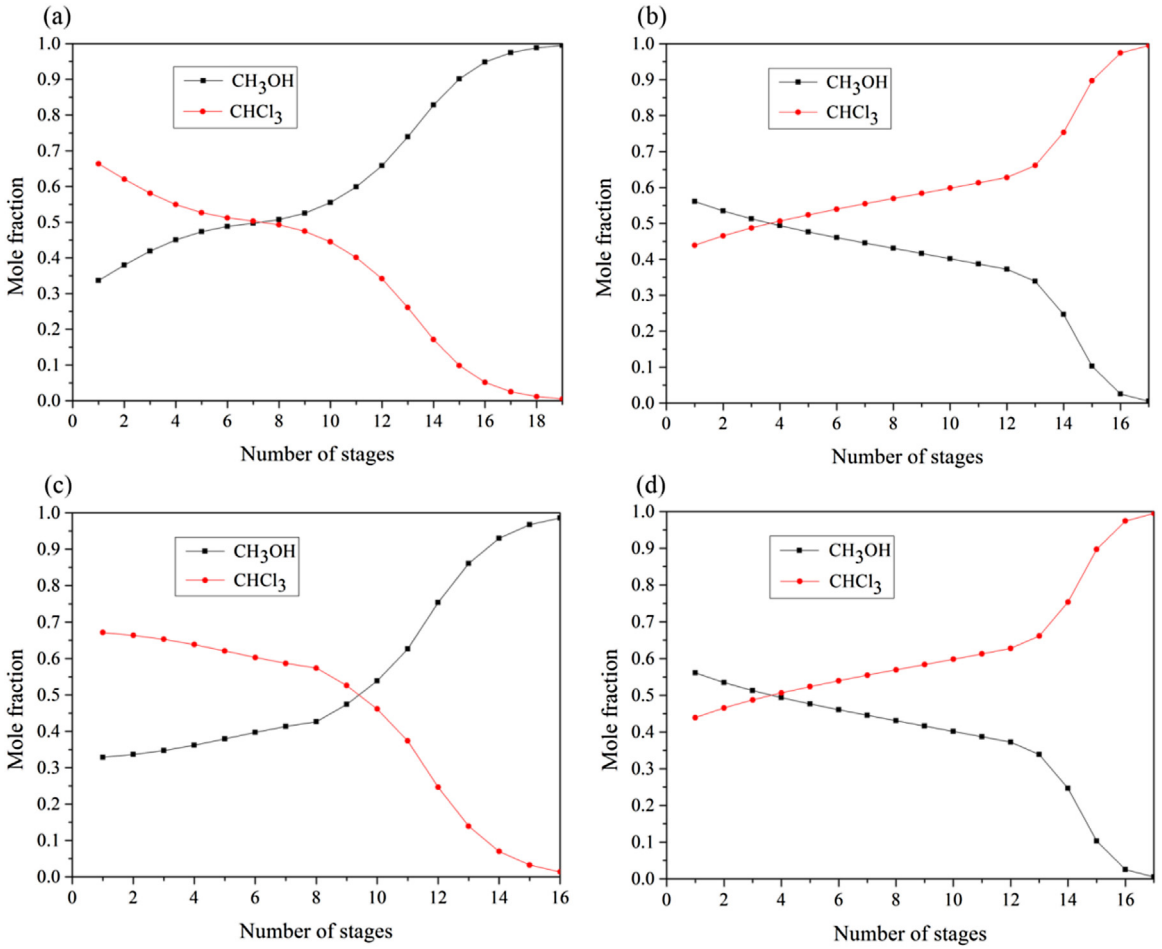

Fig. 10. Composition profiles for the methanol-chloroform system: (a) Column T1 with no heat integration. (b) Column T2 with no heat integration. (c) Column T2 with partial integration. (d) Column T2 with partial heat integration.

3.3. Results and discussion

The separation of the azeotropic mixtures of acetone/methanol and methanol/chloroform using the PSD was optimized by the proposed SAA-based optimization method. The results of the PSD process without heat integration optimized by the SAA-based optimization method were compared with those of the conventional optimization methods. For the acetone-methanol system, a 5.69% decrease with the pressure specified and a 17.32% decrease with the pressure optimized are shown. For the methanol-chloroform system, a 1.79% decrease with the pressure specified and a 9.04% decrease with the pressure optimized are shown. The results of the PSD process without heat integration show that the SAA-based optimization method can obtain a minor TAC and the even global optimum TAC, as long as the parameter settings of the SAA are reasonable.

For a general procedure for the SAA-based PSD optimization, the computing time to determine the parameter settings mainly depends on the choice of T_0 and K, which takes approximately 0.3 h. The procedure with the pressure specified takes approximately 1.0 h, and the procedure with pressure optimized takes approximately 3.0 h. The computing time of the sequential iterative optimization and the heuristic optimization method is mainly dependent on the researcher and the initial design of the PSD to a great extent. To make a comparison, we chose a range of time. For the general optimization of the PSD with the pressure specified, the computing time of the sequential iterative optimization, the heuristic optimization method and the SAA-based optimization method are 10–30 h, 2–10 h, and 1–2 h, respectively. The SAA-based optimization method achieves automatic optimization with less computing time compared with the conventional optimization methods.

The optimum design of the heat-integrated process was obtained using the SAA-based optimization method. The optimum TACs optimized by the SAA-based optimization method were compared with the optimum TACs of the solution without further optimization. For the PSD process with partial heat integration separating the acetone-methanol mixture, a 9.00% decrease with the pressure specified and a 15.52% decrease with the pressure optimized were shown. For the PSD process with full heat integration separating the methanol-chloroform mixture, a 0.40% decrease with the pressure specified and a 4.05% decrease with the pressure optimized were shown. The results show a minor TAC, and an improved design of the heat integration processes can be obtained by the SAA-based optimization method, revealing that it is necessary to use the optimization of the PSD process with heat integration rather than rely on results based on the optimum design without heat integration.

The pressures in the two columns of the PSD were optimized based on the TAC using the SAA-based optimization method. For the acetone-methanol system, the top temperature of the optimum low-pressure column is 315.6 K at 0.62 atm. For the methanol-chloroform system, the top temperature of the optimum low-pressure column is 317.8 K at 0.71 atm. For the cases

described in this paper, recycled cooling water with a temperature of approximately 305.0 K was used as the cooling medium for the low-pressure column condenser. In fact, if the top temperature of the low-pressure column is lower than 315 K, the cooling medium should be replaced with refrigerated water or another expensive cooling medium and the cost for cooling will increase. The results of these cases show that the optimization with the pressure optimized has a significant improvement over that of the pressure specified. Therefore, it is important to optimize the precise pressures in the two columns of the PSD process.

4. Conclusions

A method of design and optimization of the PSD process based on the SAA was proposed in this paper. To handle the problem of optimizing the PSD process with continuous variables and discrete variables, the move generator and cooling schedule of the SAA were discussed, and suitable parameter settings for the PSD were investigated. The cases of methanol-chloroform and acetone-methanol systems were studied. The results show that the present method can optimize the PSD process with no, partial, and full heat integrations. A SAA-based optimization process starting with different initial values of PSD design variables results in the same optimum design, which demonstrated that the global optimal design is obtained. The optimization results of the PSD process without heat integration show that an improved optimum design with a minor TAC is obtained by the SAA-based optimization method compared with those of the conventional optimization methods. The optimization results with the pressure optimized are substantially improved compared with those of the pressure specified. Therefore, this step is important for the optimization of the pressures in the two columns of PSD. The SAA-based optimization method has the advantages of automatic optimization, less computing time, and a greater chance to obtain the global optimal design. This work will be helpful to optimize the PSD processes for separating other systems.

Conflict of interest

The authors declare no competing financial interest.

Acknowledgements

The authors gratefully acknowledge the anonymous reviewers for the insightful comments and suggestions. The ideas of pressure optimization and heat integration process optimization improve the quality of this paper to a large extent. The authors also gratefully acknowledge financial support from the National Natural Science Foundation of China (Project 21306093).

Appendix A. SAAPSDO software code

```
'start SA A
Public Sub SAA()
    'Value(1) output to the specified Excel cells(i, 1)
    xlSheet.Cells(i, 1) = Value(1)
    xlSheet.Cells(i, 2) = Value(2)
...'Ellipsis of the others
    'Calcalate TAC
    TAC = CalcTAC(i)
    T0 = Val(Text1(38).Text):Tf = Val(Text1(39).Text)
    alpha = Val(Text1(40).Text):L = Val(Text1(41).Text)
    K = Text1(42).Text: j = 1: i = 1:T=T0
      Do
          Do
          'Generate new design variables
          d_new = Gen_Vars(i)
          'Calcalate TAC
          TAC_new = CalcTAC(i)
          delta = (TAC_new - TAC) / K
          Randomize
          'Metropolis Criterion
          If delta <= 0 Or Rnd() < Exp(-delta / T) Then
            TAC = TAC_new
            For d7 = 1 To 9
                VX(d7) = Value(d7)
            Next d7
          End If
        'Aspen errors TAC_new=1E+18
          If TAC_new <> 1E+18 Then
          j=j + 1 : i = i + 1
          End if
          xlSheet.Cells(i, 17) = T
          'The row of local minimum value sets blue
          xlSheet.Rows(Min(9)).Interior.Color = vbBlue
      Loop while j<= L
      T = T * alpha
      j= 1
Loop while T<= Tfreeze
... 'Ellipsis of the others
```

References

An, W.-z., Yuan, X.-G., 2009. A simulated annealing-based approach to the optimal synthesis of heat-integrated distillation sequences. Comput. Chem. Eng. 33, 199–212.

An, Y., Li, W., Li, Y., Huang, S., Ma, J., Shen, C., Xu, C., 2015. Design/optimization of energy-saving extractive distillation process by combining preconcentration column and extractive distillation column. Chem. Eng. Sci. 135, 166–178.

Aspen Plus, 2007. Aspen Plus User Guide. Aspen Technology, Massachusetts.

Bastos, P.D.A., Oliveira, F.S., Rebelo, L.P.N., Pereiro, A.B., Marrucho, I.M., 2015. Separation of azeotropic mixtures using high ionicity ionic liquids based on 1-ethyl-3-methylimidazolium thiocyanate. Fluid Phase Equilib. 389, 48–54.

Cardoso, M., Salcedo, R., De Azevedo, S.F., Barbosa, D., 2000. Optimization of reactive distillation processes with simulated annealing. Chem. Eng. Sci. 55, 5059–5078.

Chan, L.M., Srinivasan, R., 2016. A hybrid CPU-graphics processing unit (GPU) approach for computationally efficient simulation-optimization. Comput. Chem. Eng. 87, 49–62.

Cheng, J.-K., Lee, H.-Y., Huang, H.-P., Yu, C.-C., 2009. Optimal steady-state design of reactive distillation processes using simulated annealing. J. Taiwan Inst. Chem. Eng. 40, 188–196.

García-Herreros, P., Gómez, J.M., Gil, I.D., Rodríguez, G., 2011. Optimization of the design and operation of an extractive distillation system for the production of fuel grade ethanol using glycerol as entrainer. Ind. Eng. Chem. Res. 50, 3977–3985.

Gutiérrez-Antonio, C., Ojeda-Gasca, A., Bonilla-Petriciolet, A., Segovia-Hernández, J.G., Briones-Ramírez, A., 2014. Effect of using adjusted parameters, local and global optimums, for phase equilibrium prediction on the synthesis of azeotropic distillation columns. Ind. Eng. Chem. Res. 53, 1489–1502.

Hanke, M., Li, P., 2000. Simulated annealing for the optimization of batch distillation processes. Comput. Chem. Eng. 24, 1–8.

Hosgor, E., Kucuk, T., Oksal, I.N., Kaymak, D.B., 2014. Design and control of distillation processes for methanol?chloroform separation. Comput. Chem. Eng. 67, 166–177.

Kirkpatrick, S., Gelatt, C.D., Vecchi, M.P., 1983. Optimization by simulated annealing. Science 220, 671–680.

Kunnakorn, D., Rirksomboon, T., Siemanond, K., Aungkavattana, P., Kuanchertchoo, N., Chuntanalerg, P., Hemra, K., Kulprathipanja, S., James, R.B., Wongkasemjit, S., 2013. Techno-economic comparison of energy usage between azeotropic distillation and hybrid system for water–ethanol separation. Renew. Energy 51, 310–316.

Lahiri, S.K., 2014. Particle swarm optimization technique for the optimal design of plate-type distillation column. In: Applications of Metaheuristics in Process Engineering. Springer, pp. 153–182.

Li, J., Du, J., Zhao, Z., Yao, P., 2015. Efficient method for flexibility analysis of large-scale nonconvex heat exchanger networks. Ind. Eng. Chem. Res. 54, 10757–10767.

Liang, K., Li, W., Luo, H., Xia, M., Xu, C., 2014. Energy-efficient extractive distillation process by combining preconcentration column and entrainer recovery column. Ind. Eng. Chem. Res. 53, 7121–7131.

Lim, K.T., Matsumoto, H., Yamaki, T., Matsuda, K., 2014. A framework for application of genetic algorithm to model-based design of reactive distillation process. J. Chem. Eng. Jpn. 47, 187–194.

Liu, X., Zhao, C., 2012. Melt index prediction based on fuzzy neural networks and PSO algorithm with online correction strategy. AIChE J. 58, 1194–1202.

Lladosa, E., Montón, J.B., Burguet, M., 2011. Separation of di-*n*-propyl ether and *n*-propyl alcohol by extractive distillation and pressure-swing distillation: computer simulation and economic optimization. Chem. Eng. Prog. 50, 1266–1274.

Luo, H., Liang, K., Li, W., Li, Y., Xia, M., Xu, C., 2014. Comparison of pressure-swing distillation and extractive distillation methods for isopropyl alcohol/diisopropyl ether separation. Ind. Eng. Chem. Res. 53, 15167–15182.

Luyben, W.L., 2008. Comparison of extractive distillation and pressure-swing distillation for acetone-methanol separation. Ind. Eng. Chem. Res. 47, 2696–2707.

Luyben, W.L., 2013. Distillation Design and Control Using Aspen Simulation. John Wiley & Sons.

Luyben, W.L., 2014. Methanol/trimethoxysilane azeotrope separation using pressure-swing distillation. Ind. Eng. Chem. Res. 53, 5590–5597.

Mahdi, T., Ahmad, A., Nasef, M.M., Ripin, A., 2014. State-of-the-art technologies for separation of azeotropic mixtures. Sep. Purif. Rev. 44, 308–330.

Martins, F., Costa, C.A.V., 2010. Economic, environmental and mixed objective functions in non-linear process optimization using simulated annealing and tabu search. Comput. Chem. Eng. 34, 306–317.

Metropolis, N., Rosenbluth, A.W., Rosenbluth, M.N., Teller, A.H., Teller, E., 1953. Equation of state calculations by fast computing machines. J. Chem. Phys. 21, 1087–1092.

Modla, G., Lang, P., 2012. Removal and recovery of organic solvents from aqueous waste mixtures by extractive and pressure swing distillation. Ind. Eng. Chem. Res. 51, 11473–11481.

Modla, G., Lang, P., Denes, F., 2010. Feasibility of separation of ternary mixtures by pressure swing batch distillation. Chem. Eng. Sci. 65, 870–881.

Ochoa-Estopier, L.M., Jobson, M., Chen, L., Rodríguez-Forero, C.A., Smith, R., 2015. Optimization of heat-integrated crude oil distillation systems. Part II: heat exchanger network retrofit model. Ind. Eng. Chem. Res. 54, 5001–5017.

Quijada-Maldonado, E., Meindersma, G.W., de Haan, A.B., 2014. Ionic liquid effects on mass transfer efficiency in extractive distillation of water–ethanol mixtures. Comput. Chem. Eng. 71, 210–219.

Silva, H.G., Salcedo, R.R., 2011. SIMOP: Application to global MINLP stochastic optimization. Chem. Eng. Sci. 66, 1306–1321.

Skiborowski, M., Harwardt, A., Marquardt, W., 2015. Efficient optimization-based design for the separation of heterogeneous azeotropic mixtures. Comput. Chem. Eng. 72, 34–51.

Sudibyo, S., Murat, M., Aziz, N., 2015. Simulated annealing-particle swarm optimization (SA-PSO): particle distribution study and application in neural wiener-based NMPC. IEEE Control Conference (ASCC) 2015 10th Asian, 1–6.

Wang, L., Pu, Z., Wen, S., 2012. Optimal operation strategies for batch distillation by using a fast adaptive simulated annealing algorithm. IEEE Intelligent Control and Automation (WCICA) 2012 10th World Congress, 2426–2430.

Wang, Y., Zhang, Z., Zhang, H., Zhang, Q., 2015. Control of heat integrated pressure-Swing-distillation process for separating azeotropic mixture of tetrahydrofuran and methanol. Ind. Eng. Chem. Res. 54, 1646–1655.

Zhu, Y., Wen, H., Xu, Z., 2000. Global stability analysis and phase equilibrium calculations at high pressures using the enhanced simulated annealing algorithm. Chem. Eng. Sci. 55, 3451–3459.